

Article

Mathematical Model of Photodarkening in Rare-Earth-Doped Fiber

Tianran Sun ^{1,2}, Xinyang Su ^{1,2,*}, Yunhong Zhang ^{1,2}, Huaiwei Zhang ^{1,2}, Yabo Sun ^{1,2} and Yi Zheng ^{1,2}

¹ School of Physical Science and Engineering, Beijing Jiaotong University, Beijing 100044, China; 18118043@bjtu.edu.cn (T.S.); 19118047@bjtu.edu.cn (Y.Z.); 18126233@bjtu.edu.cn (H.Z.); 20121663@bjtu.edu.cn (Y.S.); yizheng@bjtu.edu.cn (Y.Z.)

² Key Laboratory of Luminescence and Optical Information, Ministry of Education, Beijing Jiaotong University, Beijing 100044, China

* Correspondence: suxinyang@bjtu.edu.cn (X.S.)

Abstract: In this paper, an improved mathematical model is proposed by taking the factors of high-energy photons and temperature into consideration, which is verified and explained by the experimental data in our experiments and other papers. By fitting and analyzing the experimental data, we can quantitatively determine the relationship between the pump power P_λ and the photon frequency ν in the fiber core, the core area A and the temperature T of the fiber core and PD loss, and explain the mechanism of the PD phenomenon to a certain extent. We believe that the excitation of color centers by high-energy photons is the main reason for photodarkening. Furthermore, there is a positive correlation between the power of high-energy photons and the photodarkening rate, and the temperature is positively correlated with the saturated photodarkening absorption.

Keywords: photodarkening; rare-earth-doped fiber; high-energy photons; mathematical model



Citation: Sun, T.; Su, X.; Zhang, Y.; Zhang, H.; Sun, Y.; Zheng, Y. Mathematical Model of Photodarkening in Rare-Earth-Doped Fiber. *Photonics* **2022**, *9*, 370. <https://doi.org/10.3390/photonics9060370>

Received: 25 April 2022

Accepted: 23 May 2022

Published: 25 May 2022

Publisher's Note: MDPI stays neutral with regard to jurisdictional claims in published maps and institutional affiliations.



Copyright: © 2022 by the authors. Licensee MDPI, Basel, Switzerland. This article is an open access article distributed under the terms and conditions of the Creative Commons Attribution (CC BY) license (<https://creativecommons.org/licenses/by/4.0/>).

1. Introduction

In 1988, Millar et al. [1] first discovered the phenomenon of photodarkening (PD) in Tm-doped quartz fiber, and the effect of PD has attracted wide attention since. PD is an important problem in fiber lasers. The characteristic of PD is broadband absorption centered on the wavelength of visible light. The performance of PD is also related to the preparation method of active fiber [2–7]. The darkening is a process of continuous competition between PD and bleaching. PD is considered to be the relaxation process of a statistical ensemble of micro-optical centers (PD precursor). These micro-optical centers reversibly absorb the energy of high-energy photons and convert it into color centers (CCs), resulting in additional PD-induced loss [8]. CCs can lead to additional absorption of a wide spectrum centered on visible light, which reduces the power conversion efficiency of the fiber laser and generates excess heat in the fiber laser [9,10].

High-energy photons directly interact with the fiber through the photoelectric effect, Compton scattering and electron pair effect result in the ionization of electron–hole pairs in the fiber. When electron–hole pairs are captured by intrinsic defects, doping defects, impurity defects, and radiation-induced defects in fiber, a special point defect with an effective charge will be formed. This defect will combine electrons and holes, resulting in light absorption in the fiber. Because its absorption band usually falls within the visible light range, it is called the color center (CC) [11,12].

In 2018, Röpke et al. [13] present a stretched exponential model of PD-induced loss. In their model, the PD effect is treated as the relaxation process of the statistical ensemble of micro-optical centers (PD complexes). These micro-optical centers (PD complexes) are reversibly converted into CCs by the energy of pumping photons, resulting in measurable PD loss. The next year, S. Jetschke et al. [14] from the same institute further improved and verified the model. The PD parameters determined by fitting the measured curves

with the stretched exponential function are linked to the activation and deactivation rates of micro-optic centers (PD complexes). They linked the variation of the PD rate and the equilibrium loss with pump power and inversion, and established a mathematical model. However, this led to problems. According to [15,16], many PD phenomena are not directly excited by the pump power, but are caused by CCs excited by high-energy photons which are formed by a series of upconversion processes through pump power. Even the undoped fiber can absorb X-rays and 200–220 nm ultraviolet rays and produce CCs [11]. Therefore, to a certain extent, the inversion is not directly related to the PD phenomenon, but related to the high-energy photons formed in the upconversion process induced by pump power.

In this paper, an improved mathematical model is proposed by taking the factors of high-energy photons and temperature into consideration, and a physical quantity σ is introduced by imitating the absorption and emission cross-sectional area in the laser energy level system. It is also verified and explained through some experimental results. In addition, fitting analysis shows that the PD rate is related to the high-energy photons generated by pump power upconversion, and it is proved that the temperature can significantly affect maximum additional loss. Finally, we describe the PD experiment of Tm-doped photonic crystal fiber, and further verify the fitting relationship between the maximum additional loss and temperature, providing the additional absorption spectrum caused by PD.

2. Photodarkening Mechanism

As we all know, high-energy photons will produce CCs in matrices such as quartz glass, which leads to absorption bands [15,16], and ultraviolet can also be used to inscribe fiber Bragg gratings [17]. Therefore, CCs will appear in the optical fiber by using an ultraviolet laser [18] or even an ultraviolet lamp [19,20]. The oxygen-deficient center (ODC) in the germanosilicate glass fiber will release free electrons when irradiated by a 240 nm light. The released free electrons are trapped near the GeO_4 tetrahedron, forming a Ge (I) CC with an absorption peak at 280 nm and an absorption spectrum range extending to the near-infrared band, showing an obvious PD phenomenon [20]. In Yb-doped aluminosilicate glass, a charge transfer (CT) band appears near 230 nm and the conversion of Yb^{3+} ions from trivalent state to low valence state Yb^{2+} [4,19,21–25]. When stable Yb^{2+} is formed, free holes are generated and excited to a higher energy level CT state, which leads to the formation of CCs, resulting in additional losses at ultraviolet and infrared wavelengths [21,26,27]. Even undoped glass can absorb X-rays and 200–220 nm ultraviolet rays to produce CCs, which will greatly reduce the transmittance of the glass [11].

To sum up, we believe that when the laser works normally in an ordinary environment, the CC is generated by the interaction between high-energy (short-wavelength) photons and ions, atoms, or electrons in the crystal. This means that not all wavelengths leading to PD (especially long waves) are directly involved in the generation process of CCs, and the conversion process from low-energy photons to high-energy photons needs to be performed first. In addition, there are different ways of generating high-energy photons in a laser, mainly including excited-state absorption (ESA) [28], energy transfer upconversion (ETU) [29], avalanche upconversion [29], and cooperative luminescence [30–32].

Due to the complex energy level structure of Tm ions, Tm ions are very easy to up-convert the infrared pump light into blue and ultraviolet light [33,34]. The blue light was observed in Tm-doped fiber pumped by laser sources ranging from 1.06 to 1.14 μm [5,28,35–37], which is the $^1\text{G}_4$ – $^3\text{H}_6$ transition of Tm ions produced by three-photon absorption. Through avalanche upconversion and ETU, pumping with the wavelength of 790 nm can also produce blue light in Tm-doped fiber [29]. This conclusion is also confirmed in our experiment, which shows the spectrum of Tm-doped fiber pumped by laser at 793 nm in Figure 1. It is known that Tm ions with $^1\text{G}_4$ level exhibit a strong absorption band at approximately 488 nm and Tm ions at $^1\text{G}_4$ level can be excited to $^1\text{I}_6$ – $^3\text{P}_0$ levels by excited-state absorption (ESA), so as to upconvert 488 nm radiation to ultraviolet source [38].

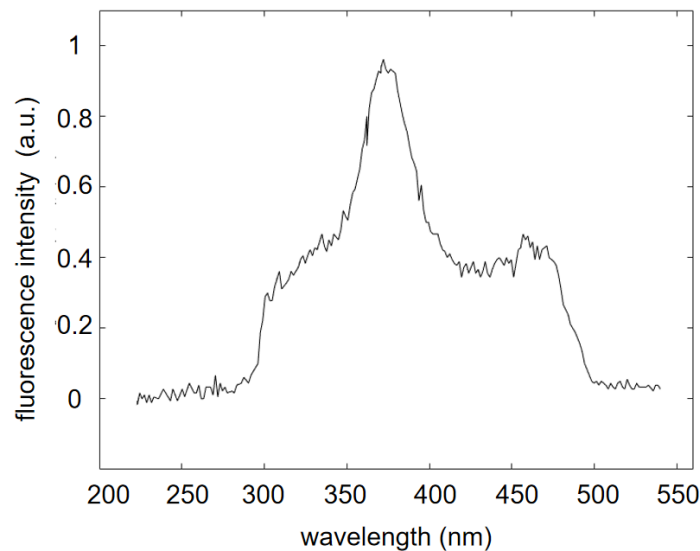


Figure 1. The spectrum of Tm-doped fiber pumped by laser at 793 nm.

Compared with the Tm ion, the energy level structure of the Yb ion is simple. ESA or the upconversion process cannot be used to explain the process of generating high-energy photons in Yb-doped fiber lasers. However, the evidence shows that there are trace Tm ions in Yb-doped fibers, which has a great influence on the PD generation process in Yb-doped fiber [39]. Under the condition of the high-power pump Yb-doped fiber with a wavelength of 977 nm, the cluster composed of three or four Yb ions can emit ultraviolet radiation. Through cooperative luminescence, 500 nm radiation is produced by the simultaneous de-excitation of two cluster ions emits [30]. In addition, some intrinsic defects in the fiber can also absorb the pump power and produce high-energy photons [7]. In the process of generating PD, the above processes are not independent and need to work together [40].

3. Model

Darkening is a process of continuous competition between PD and bleaching. In this paper, a semi-empirical formula for the PD and bleaching process is established by imitating a two-level laser system, as shown in Figure 2.

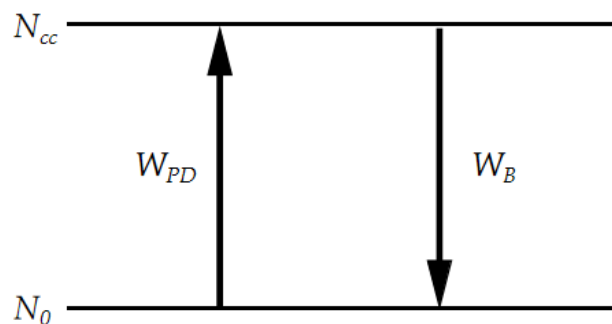
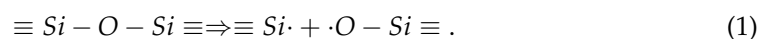


Figure 2. The process of photodarkening and bleaching. N_0 is the density of the photodarkening precursor, N_{cc} is the density of the CCs, W_{PD} is the photodarkening rate, and W_B is the bleaching rate.

In Figure 2, $N_0(t)$ is the density of PD precursor that can produce CCs by photoionization. Take E^{\prime} - centers ($\equiv Si\cdot$), for example. E^{\prime} - centers are generated in the following way [41,42]



The $\equiv Si - O - Si \equiv$ is the PD precursor that can form CC. The generation rate of the density of the CCs can be expressed as

$$\frac{dN_{cc}}{dt} = W_{PD}N_0(t) - W_B N_{cc}(t) \tag{2}$$

$$N_0(t) + N_{cc}(t) = N_0(0), \tag{3}$$

where $N_{cc}(t)$ is the density of CCs varying with time t , and W_{PD} and W_B are the rate of PD and bleaching; therefore, we assume

$$W_{PD} = \frac{P_\lambda(z)\varphi(r,\phi)}{Ah\nu}\sigma_{N_0} \tag{4}$$

$$W_B = \frac{P_\lambda(z)\varphi(r,\phi)}{Ah\nu}\sigma_{N_{cc}} + Q(T), \tag{5}$$

where P_λ is the launched high-energy photon power in the core of the fiber. A is the core area. h is the Planck constant. ν is the photon frequency. $\varphi(r,\phi)$ is the normalized signal profile σ_{N_0} is the probability that the PD precursor of unit density is excited by one photon. $\sigma_{N_{cc}}$ is the probability that CC of unit density is excited by one photon. $Q(T)$ is the temperature-dependent thermal bleaching rate. Then, the density of CCs can be obtained by Formula (2)

$$N_{cc}(z,r,\phi,T,t) = \int_0^t \frac{dN_{cc}}{dt} dt = \int_0^t [W_{PD}N_0(t) - W_B N_{cc}(t)] dt \tag{6}$$

It is assumed that the extra absorption caused by the CC is directly proportional to the density of the CCs, therefore we assume

$$\alpha_{PD}(t) = \alpha_\lambda N_{cc}(t), \tag{7}$$

where α_λ is the additional absorption coefficient at wavelength λ generated by the CC of unit density. $\alpha_{PD}(t)$ can be obtained from the measurement of the PD loss experiment. α_λ is measured by preparing a CC sample of known density. $Q(T)$ can be obtained by a thermal bleaching experiment. $\sigma_{N_{cc}}$ and σ_{N_0} can be obtained by bringing in Formulas (6) and (7) with the above parameters.

By using a stretched exponential formalism with time-dependent rate coefficients, Formula (1) describing the change in the density of the CC will be rewritten as [43,44]

$$\frac{dN_{cc}}{dt} = \beta t^{\beta-1} W_{PD}^\beta N_0(t) - \kappa t^{\kappa-1} W_B^\kappa N_{cc}(t) \tag{8}$$

where β and κ are the stretching parameters for photodarkening and photobleaching. The stretching parameter β and κ was found to depend on the fiber type. When the pump wavelength is far away from the wavelength where photobleaching can occur and the core temperature is not enough to produce thermal bleaching, bleaching can be ignored, and the formula can be rewritten as

$$\frac{dN_{cc}}{dt} = \beta t^{\beta-1} W_{PD}^\beta [N_{cc,max}(T) - N_{cc}(t)], \tag{9}$$

where $N_{cc,max}(T)$ is the final equilibrium state of the density of the CCs related to the core temperature [7,45]. Temperature is used to describe the degree of thermal movement of microparticles, which has an important impact on the stability of PD precursors and CCs. Integrate Formula (9) to obtain the stretched exponential function,

$$N_{cc}(t) = N_{cc,max}(T) \left\{ 1 - \exp \left[-(W_{PD}t)^\beta \right] \right\} \tag{10}$$

Therefore, we can obtain the formula of additional absorption of PD through Formulas (7) and (10)

$$\begin{aligned} \alpha_{PD}(t) &= \alpha_{\lambda} N_{cc,max}(T) \left\{ 1 - \exp \left[-(W_{PD}t)^{\beta} \right] \right\} \\ &= \alpha_{PD,max}(T) \left\{ 1 - \exp \left[-(W_{PD}t)^{\beta} \right] \right\}, \end{aligned} \tag{11}$$

where $\alpha_{PD,max}(T)$ is the maximum additional loss, W_{PD} is the PD rate. It can be seen from the formula that the additional loss $\alpha_{PD}(t)$ is the stretched exponential function of the maximum additional loss $\alpha_{PD,max}(T)$ and the PD rate W_{PD} .

If the specific value of $N_{cc,max}(T)$ and the curve of additional loss caused by photodarkening under a certain power with time can be provided, σ_{N_0} can be obtained through Equations (4) and (11). When σ_{N_0} is obtained, the time-dependent curve of additional loss caused by photodarkening at different power levels can be predicted by Formulas (4) and (11).

4. Data Simulation

We digitize the experimental data in other research papers about PD under different pump powers and use the above mathematical model for verification and interpretation.

In 2007, Koponen et al. [7] conducted PD rate measurement experiments using two different Yb-doped fibers. The length of the sample fiber is 0.1 m, the probe light wavelength is 633 nm, the pump light wavelength is 920 nm, and the maximum power is 10 W.

We digitize their experimental data, and convert the original transmission into additional loss (dB/m) at different pump powers, and fit it with Formula (11). As shown in Figure 3, the colorful lines are plotted with experimental data, while the black lines are plotted with fitting data.

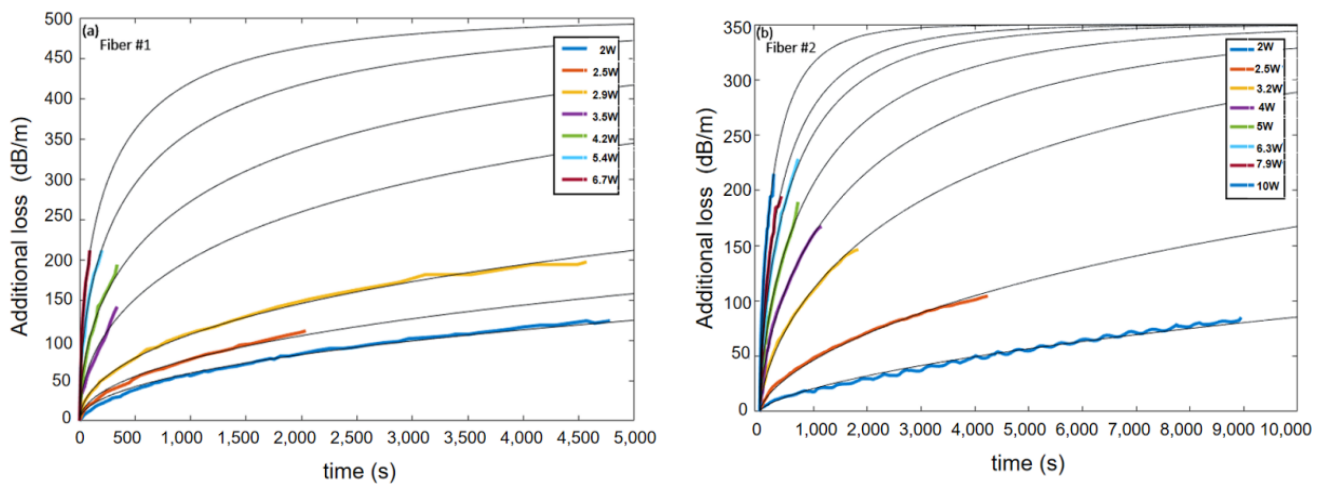


Figure 3. (a) Measurement and fitting results of Fiber #1. (b) Measurement and fitting results of Fiber #2.

Since a water-cooling device is used in the experimental device to control the core temperature and the data after loss saturation is not provided in the original paper, the maximum additional loss is set to a constant value. For optical Fiber #1, when the maximum additional loss $\alpha_{PD,max}(T)$ is equal to 500 dB/m and stretching parameters β is equal to 0.512, the calculated PD rates W_{PD} under different pump powers and coefficient of determination R^2 are shown in Table 1.

Table 1. Calculated PD rates under different pump powers of Fiber #1.

Fiber #1	2 W	2.5 W	2.9 W	3.5 W	4.2 W	5.4 W	6.7 W
W_{PD} (s^{-1})	1.75×10^{-5}	3.01×10^{-5}	6.23×10^{-5}	2.71×10^{-4}	6.25×10^{-4}	1.58×10^{-3}	3.25×10^{-3}
R^2 (%)	99.18	99.09	99.75	97.22	98.84	99.26	99.82

For optical Fiber #2, when the maximum additional loss $\alpha_{PD,max}(T)$ is equal to 350 dB/m and stretching parameters β is equal to 0.66, and the calculated PD rates and coefficient of determination R^2 under different pump powers are shown in Table 2.

Table 2. Calculated PD rates of different pump powers of Fiber #2.

Fiber #2	2 W	2.5 W	3.2 W	4 W	5 W	6.3 W	7.9 W	10 W
W_{PD} (s^{-1})	1.46×10^{-5}	5.22×10^{-5}	2.32×10^{-4}	4.74×10^{-4}	8.33×10^{-4}	1.42×10^{-3}	1.93×10^{-3}	3.56×10^{-3}
R^2 (%)	99.15	99.72	99.72	99.57	99.56	99.68	99.12	99.26

According to Formula (4), the W_{PD} is positively proportional to the high-energy photon power P_λ in the core. The logarithmic coordinate curve between the W_{PD} and the pump power (920 nm) is shown in Figure 4, in which the discrete points are the experimental data and the straight lines are the fitting curve.

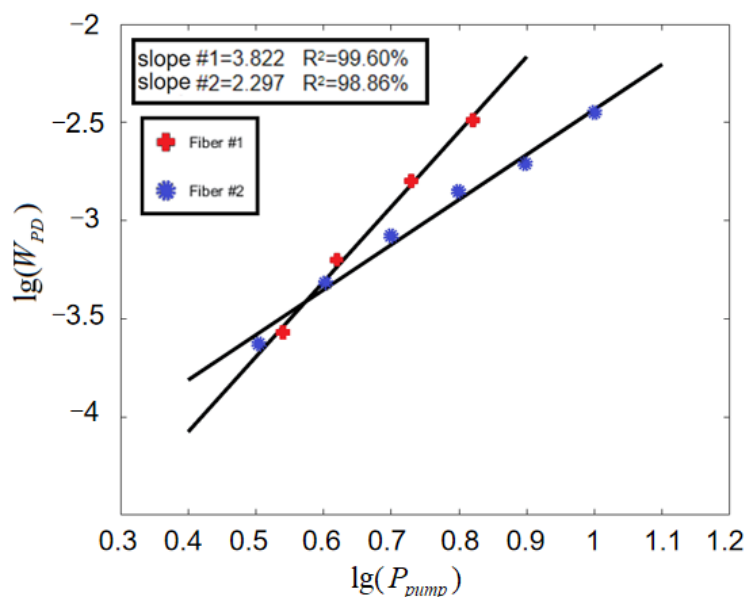


Figure 4. Logarithmic relationship between W_{PD} and P_{pump} .

When the pump power is low, the linearity of the logarithmic relationship between W_{PD} and P_{pump} is poor, and the deviation between the experimental data and the fitting curve is large. When the pump power is high, the logarithmic relationship between them tends to be stable, and the linearity gradually appears. The analysis shows that when the power is low, the particle number distribution in the fiber is complex and various multiphoton processes will occur. When the power is high, the particle number distribution is gradually stable, and the energy transition channel is also stable. Therefore, we only fit the data obtained under the condition of the high-power pump (>3.2 W). The slope of the logarithm curve of W_{PD} of Fiber #1 and Fiber #2 under higher P_{pump} is 3.822 and 2.297. Since the W_{PD} is directly proportional to the P_λ participating in PD according to Formula (4), the P_λ is directly proportional to the 3.822 and 2.297 powers of the P_{pump} in Fiber #1 and #2, respectively. Therefore, the PD of Fiber #1 can be interpreted as a four-photon process. Figure 5 is a simplified diagram of Yb^{3+} and Tm^{3+} energy levels in fiber.

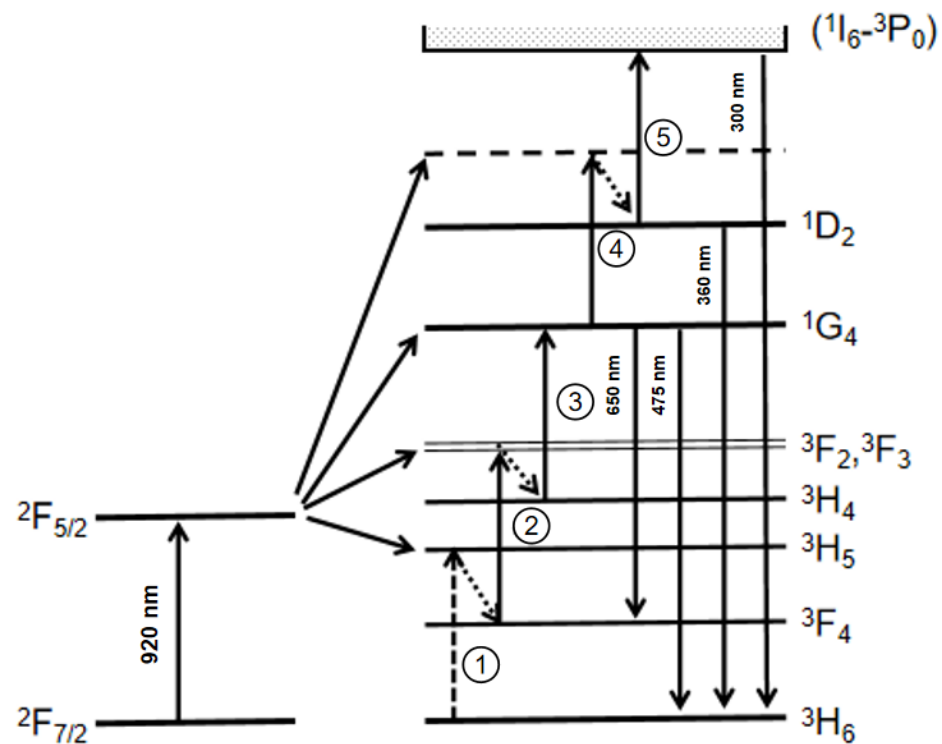


Figure 5. Schematic diagram of Yb³⁺ and Tm³⁺ energy levels in fiber.

Because the concentration of Tm³⁺ in TDF is minimal and the absorption cross-sectional area of Yb³⁺ is large, almost all the energy of the pump is absorbed by Yb³⁺, and then the energy will be transferred to Tm³⁺ energy level, to form an upconversion transition channel. Under the pump laser with the wavelength of 920 nm, Yb³⁺ in the ground state is excited to the 2F_{5/2} level, and the energy is transferred to a nearby Tm³⁺ in the ground state through energy transfer to excite it to the 3H₅ level. Because the lifetime of 3H₅ level is very short, it will be transitioned to 3F₄ level without radiation soon. Another Yb³⁺ in the excited state excites Tm³⁺ from 3F₄ to 3F₂ and 3F₃ levels through energy transfer. Through repeating the above steps, Tm³⁺ is excited to a higher energy level [46].

For Fiber #2, the P_λ in the core is approximately the square of P_{pump} . Therefore, we assume that high-energy photons are generated by the frequency doubling of the pump laser.

In 1995, Laperle et al. [5] reported the photoinduced absorption of four different Tm-doped ZBLAN fibers under a 1.12 μm laser. They used a 1.12 μm Nd: YAG laser as the pump and a 488 nm argon-ion laser as the probe to monitor the evolution of PD. The small probe light (2 μW) mixed with noise such as pump and ASE is amplified and extracted by a lock-in amplifier. The parameters of four different ZBLAN fibers are shown in Table 3.

Table 3. The parameters of four different ZBLAN fibers.

Fiber	Thulium Concentration (Parts in 10 ⁶)	Core Diameter (μm)	Numerical Aperture
A	500	3	0.21
B	1000	3	0.21
C	1000	1.7	0.39
D	11,700	3	0.21

We also digitized their experimental data, and converted the original transmission into additional loss (dB/m) at different pump powers, and fitted it with Formula (11). As shown in Figure 6. The colorful lines are the plotted experimental data while the black lines are plotted by fitting data.

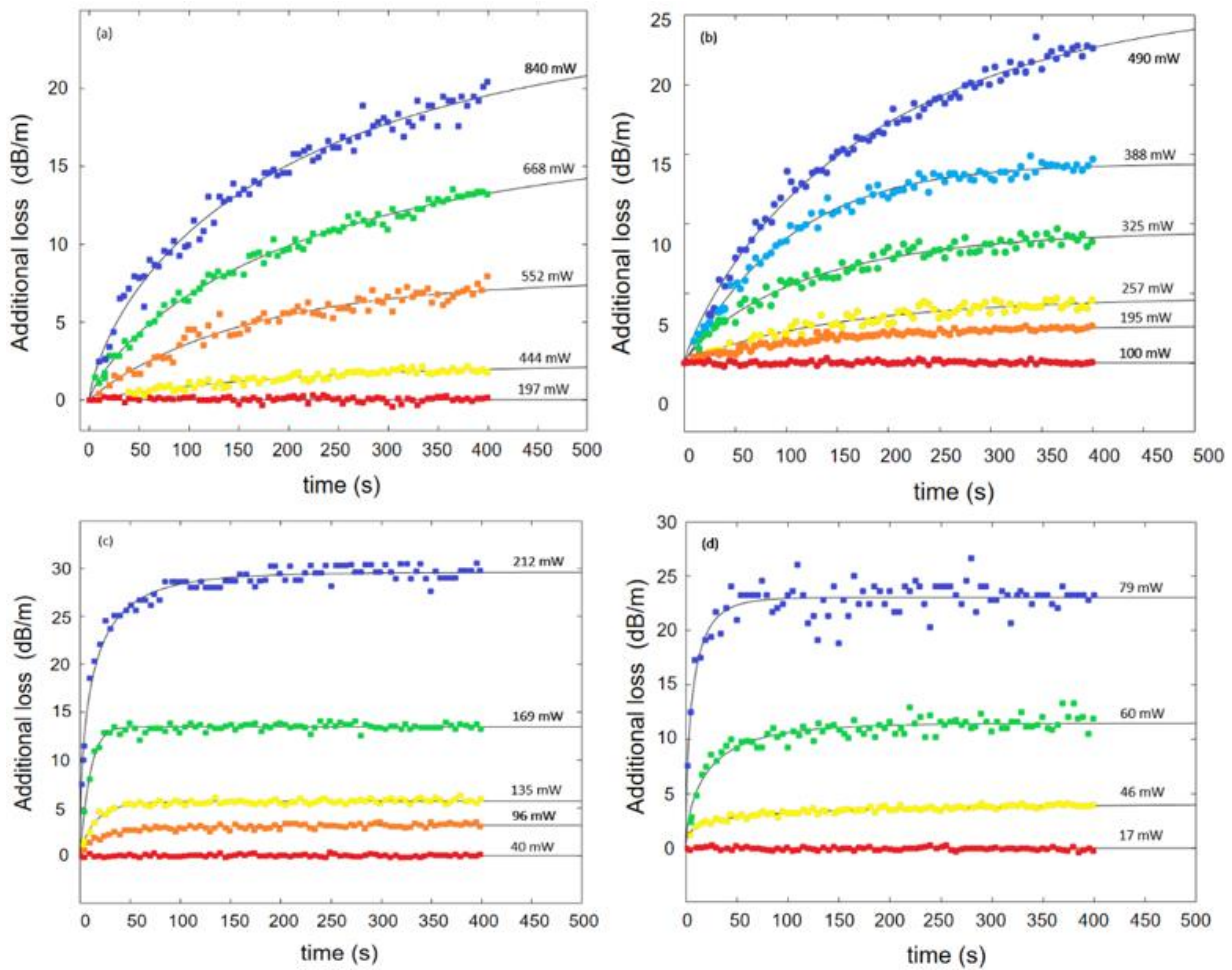


Figure 6. Measurement and fitting results of (a) Fiber A, (b) Fiber B, (c) Fiber C and (d) Fiber D.

Because the fitting results of Fibers A–C show that no matter how the pump power varies, W_{PD} is almost unchanged. Therefore, we speculate that the low doping concentration of thulium in Fibers A–C makes the upconversion of the 1.12 μm pump laser impossible to produce high-energy photons, leading to photodarkening. However, according to [4,47], a 488 nm laser can lead to photodarkening. Therefore, we speculate that the photodarkening is caused by the 488 nm probe laser, and the very low power (2 μW) of the 488 nm probe laser just explains the very small and constant photodarkening rate W_{PD} of Fibers A–C. For Fibers B and C, their Tm^{3+} concentrations are the same but their core diameters are different. It can be seen from Formula (4) that the W_{PD} is inversely proportional to the core area A . In addition, the smaller the A , the higher the energy density of the pump, and then more launched power is prone to upconversion, which explains that the W_{PD} of Fiber C is greater than that of Fiber B. The average value of the W_{PD} of Fibers A–C is shown in Table 4.

Table 4. The average value of W_{PD} of optical Fibers A–C.

Fiber	A	B	C
W_{PD}	4.939×10^{-3}	7.431×10^{-3}	7.021×10^{-2}

Since the Tm^{3+} concentration of Fiber D is one order of magnitude higher than that of other sample fibers, a great upconversion phenomenon occurs in the fiber, and the slope of the logarithmic curve of W_{PD} versus P_{pump} of Fiber D is 3.068. Therefore, the PD phenomenon of Fiber D can be explained as a three-photon process. Figure 7 is a logarithmic diagram of optical Fiber D. The W_{PD} of Fiber D at the power of 46, 60, and 79 mW is 0.02544,

0.04277, and 0.1328 s^{-1} , respectively. In addition, since almost no photodarkening occurs below the pump power of 17 mW, this set of data are abandoned in plotting. According to the above data, when the pump power of the Fiber D experiment is much lower than that of other fiber experiments, W_{PD} is also much higher than that of other fiber experiments. Therefore, we speculate that because the Tm^{3+} concentration of Fibers A–C is too low, it is difficult for high-energy photons to be generated by upconversion of pump happening in Tm ion, and the light involved in PD is 488 nm probe laser rather than $1.12 \mu\text{m}$ pump laser. Furthermore, the probe power is very low ($2 \mu\text{W}$), which just explains the W_{PD} of Fiber D is much higher than that of Fibers A–C.

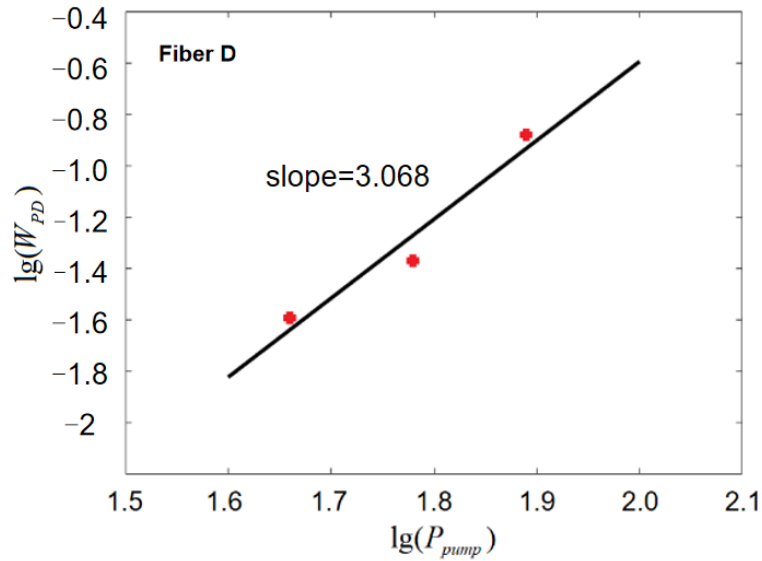


Figure 7. Logarithmic relationship between PD rate and pump power of Fiber D.

According to Formula (11), the $\alpha_{PD,max}(T)$ is related to the core temperature T . Since there is no temperature control device in the experiment, the main heat source is from the pump. From Figure 8, T is found to have a positive correlation with $\alpha_{PD,max}(T)$. T is calculated by the finite element method.

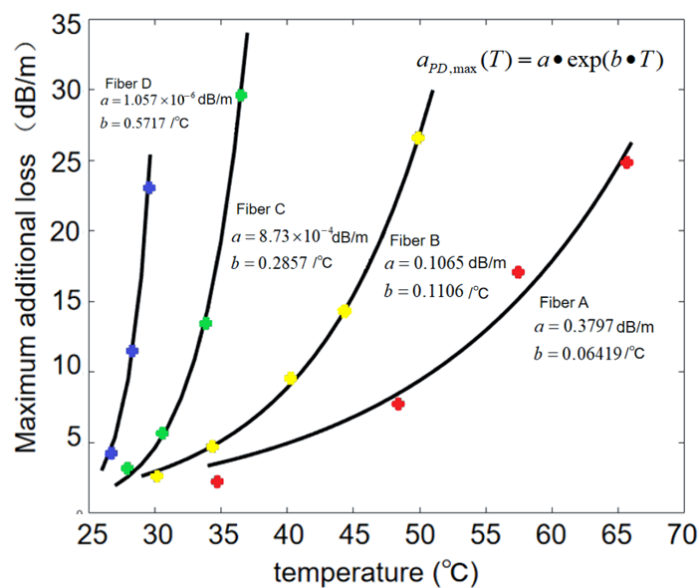


Figure 8. Relationship between core temperature and maximum additional loss. a and b in the figure is the fitting parameter.

Similar results are also obtained from [48]. In 2005, Koponen et al. measured the variation of additional loss with time under different pump powers in a Yb-doped fiber.

We digitized their experimental data, and converted them into the additional loss of the sample fiber (1 m) at different P_{pump} , and fitted it with Formula (11), as shown in Figure 9. We also found that T is directly proportional to $\alpha_{PD,max}(T)$ (Figure 10).

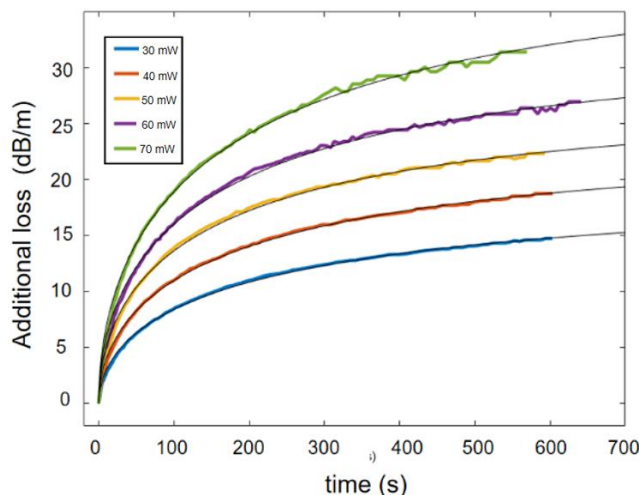


Figure 9. Additional loss under different pump power.

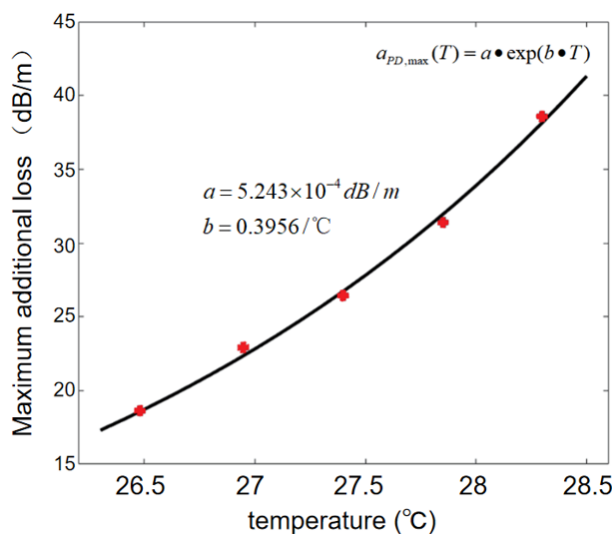


Figure 10. Relationship between core temperature and maximum additional loss. a and b in the figure is the fitting parameter.

5. Photodarkening Experiment

The PD loss and absorption spectrum are measured using the settings shown in Figure 11. A probe laser at 532 nm or white light is coupled to a self-made Tm-doped photonic crystal fiber (PCF). The two ends of the sample optical fiber are spliced with the transmission fiber. The 793 nm pump light is coupled into the sample fiber by a beam combiner, and the probe light or white light is measured through a power meter and spectrometer. The sample fibers are self-made Tm-doped PCF (the doping concentration of thulium ion is 0.075 mol%) with a 28.3 μm core diameter and an octagonal inner cladding diameter of 274.2 μm . In order to ensure the same degree of darkening in the sample fiber, the length of the fiber sample was 10 cm long (Figure 12). With this experimental device, by turning on/off the probe and the white light source (WLS) and switching the power meter (PM) and the

spectrometer (OSA) mutually, it can be freely switched between the additional loss measuring device and the absorption spectrum measuring device at a characteristic wavelength.

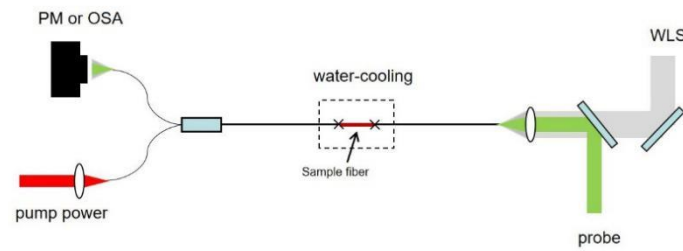


Figure 11. Setup for the pump-probe and the absorption spectrum experiment. PM, power meter; OSA, spectrometer; WLS, white light source.

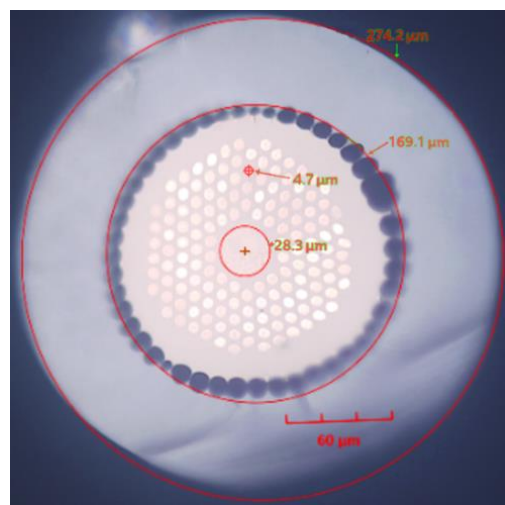


Figure 12. Microscopic image of Tm-doped photonic crystal fiber end face.

Through the experimental device, we obtained the curve of additional loss with time under different power levels (Figure 13) and fit it with Formula (11).

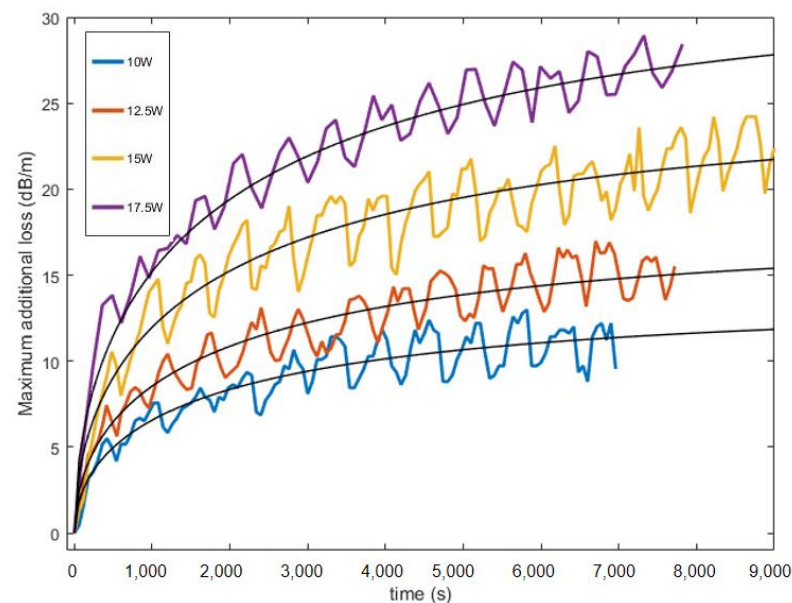


Figure 13. The curve of additional loss with time under different power levels.

When the β is equal to 0.5396, the calculated $\alpha_{PD,max}(T)$, W_{PD} and R^2 of different pump powers are shown in Table 5.

Table 5. Calculated $\alpha_{PD,max}(T)$, W_{PD} and R^2 of different pump powers of DCF.

P_{pump}	10 W	12.5 W	15 W	17.5 W
$\alpha_{PD,max}(T)$ (dB/m)	13.26	17.23	24.42	31.43
W_{PD} (s ⁻¹)	4.953×10^{-3}	4.964×10^{-3}	4.81×10^{-3}	4.645×10^{-3}
R^2 (%)	84.14	89.09	88.66	94.96

From the above data, we can see that the photodarkening rates (W_{PD}) under different powers in the experiment are almost the same. It is thought that because the P_{pump} is too high, the P_λ obtained by upconversion has reached saturation, so the W_{PD} is almost unchanged. By simulating the core temperature under different power levels, we also find the exponential relationship between T and $\alpha_{PD,max}(T)$ (Figure 14).

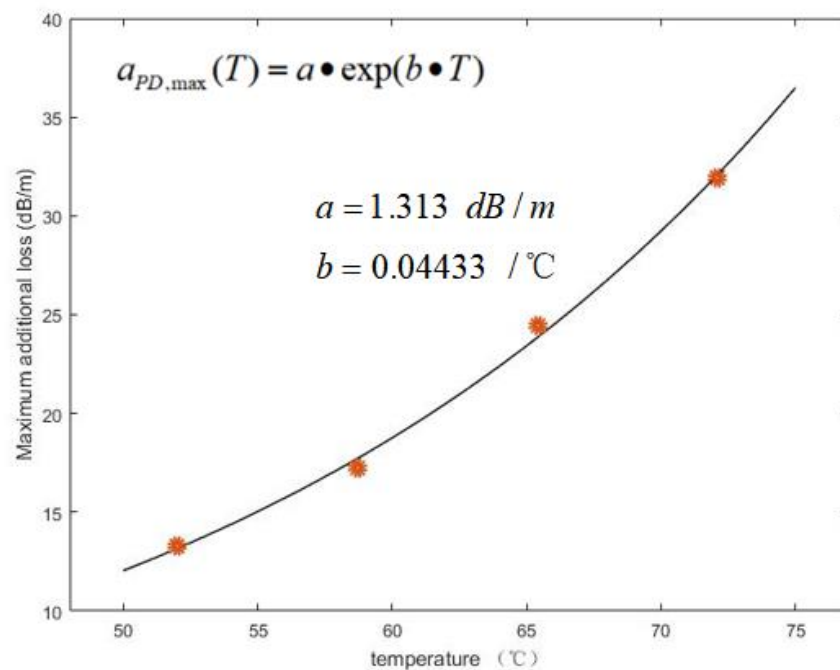


Figure 14. Relationship between core temperature and maximum additional loss. a and b in the figure is the fitting parameter.

The periodic fluctuation of the curve in Figure 13 is caused by the jittering of water-cooling temperature. When the temperature of the water cooler used in this experiment is set to be 15 °C, the real temperature will fluctuate periodically between 12 and 15 °C in a cycle of approximately 9 min, which is consistent with the fluctuation of additional loss. As can be seen from Figure 15, the additional loss increases in real time with the rise in temperature.

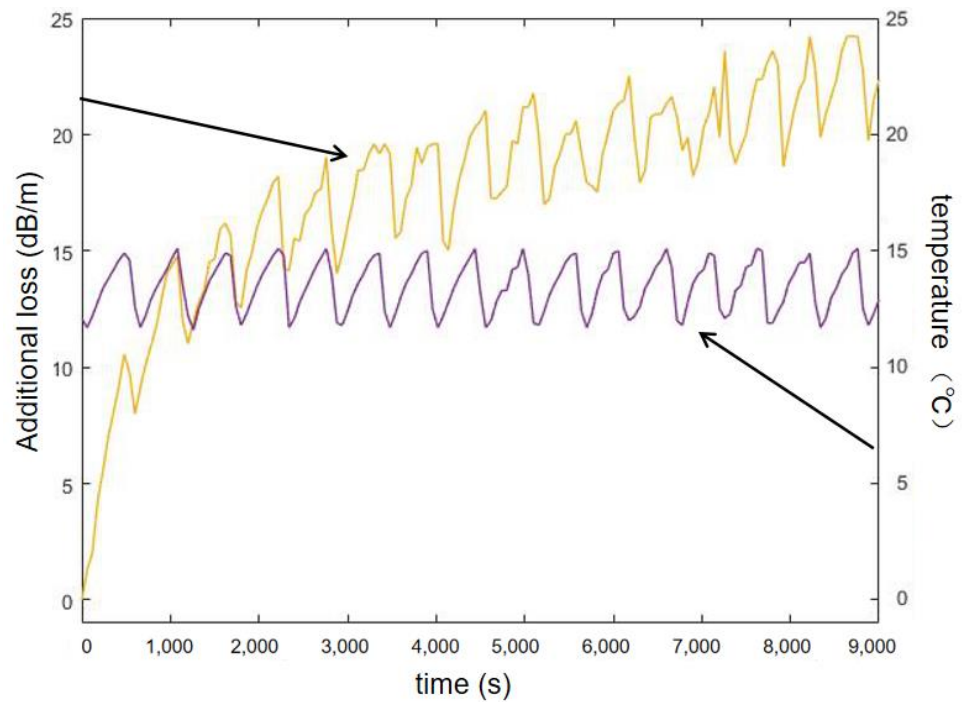


Figure 15. The curve of additional loss and water-cooling temperature with time.

By measuring the transmission spectrum of the white light passing through it before and after PD, respectively, and subtracting the transmission spectrum after PD from the transmission spectrum before PD, the absorption spectrum of the sample PCF can be obtained. The results are shown in Figure 16. The absorption spectrum shows that the color center produced by the sample PCF has strong absorption in the visible range, and the highest peak is at 579.6 nm.

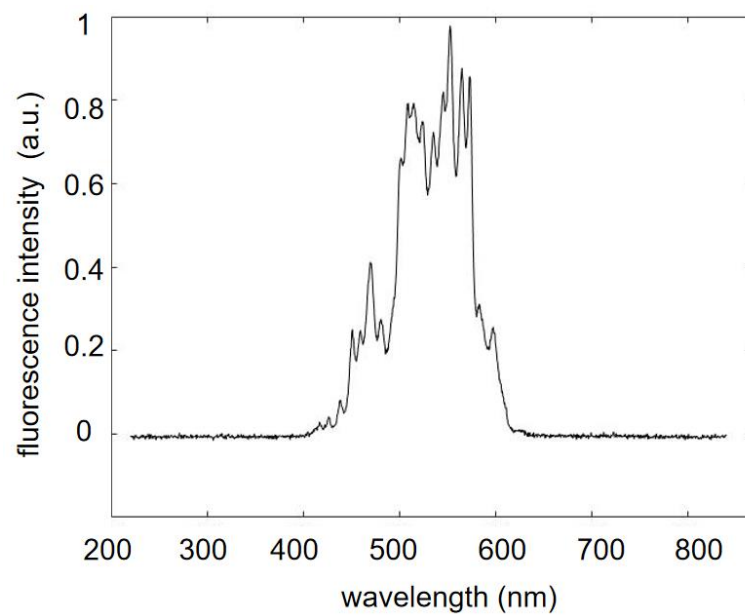


Figure 16. Photodarkening absorption spectrum of sample DCF.

6. Conclusions

An improved mathematical model for simulating and fitting the PD phenomenon is proposed by considering the factors of high-energy photons and temperature. Through fitting and analyzing the experimental data, we can quantitatively determine the relationship between different experimental parameters and PD-induced loss, and explain the mechanism of the PD phenomenon to a certain extent. It is considered that the maximum additional loss is a parameter related to the core temperature in our mathematical model, and it rises with the increase in temperature. The PD rate is directly proportional to the high-energy photon power, and the probability of exciting the unit density PD precursor by one photon, and inversely proportional to the core area. The PD phenomenon is an important problem in fiber lasers. Therefore, establishing an accurate and effective PD mathematical model is an important means to understand and suppress the PD phenomenon. However, this model still needs more comprehensive and targeted experiments for verification.

Author Contributions: Conceptualization, Y.Z. (Yi Zheng) and T.S.; investigation, X.S., Y.Z. (Yunhong Zhang) and H.Z.; writing—original draft preparation; writing—review and editing, X.S. and T.S.; visualization, X.S. and Y.S. All authors have read and agreed to the published version of the manuscript.

Funding: National Natural Science Foundation of China (61735005, 61925010); Natural Science Foundation of Beijing Municipality (4182054, 4212052); Fundamental Research Funds for the Central Universities (2021RC206).

Institutional Review Board Statement: Not applicable.

Informed Consent Statement: Not applicable.

Data Availability Statement: The data presented in this study are available on request from the corresponding author.

Conflicts of Interest: The authors declare no conflict of interest.

References

1. Millar, C.A.; Mallinson, S.R.; Ainslie, B.J.; Craig, S.P. Photochromic Behavior of Thulium-Doped Silica Optical Fibers. *Electron. Lett.* **1988**, *24*, 590–591. [[CrossRef](#)]
2. Chavez, A.D.G.; Kir'Yanov, A.V.; Barmenkov, Y.O.; Il'Ichev, N.N. Reversible photo-darkening and resonant photo-bleaching of Ytterbium-doped silica fiber at in-core 977-nm and 543-nm irradiation. *Laser Phys. Lett.* **2007**, *4*, 734–739. [[CrossRef](#)]
3. Manek-Hönninger, I.; Bouillet, J.; Cardinal, T.; Guillen, F.; Salin, F. Photodarkening and photobleaching of an ytterbium-doped silica double-clad LMA fiber. *Opt. Express* **2007**, *15*, 1606–1611. [[CrossRef](#)] [[PubMed](#)]
4. Yoo, S.; Basu, C.; Boyland, A.J.; Sones, C.; Nilsson, J.; Sahu, J.K.; Payne, D. Photodarkening in Yb-doped aluminosilicate fibers induced by 488 nm irradiation. *Opt. Lett.* **2007**, *32*, 1626–1628. [[CrossRef](#)]
5. Laperle, P.; Chandonnet, A.; Vallee, R. Photoinduced absorption in thulium-doped ZBLAN fibers. *Opt. Lett.* **1995**, *20*, 2484. [[CrossRef](#)]
6. Koponen, J.J.; Söderlund, M.; Hoffman, H.J.; Tammela, S.K. Measuring photodarkening from single-mode ytterbium doped silica fibers. *Opt. Express* **2006**, *14*, 11539. [[CrossRef](#)]
7. Koponen, J.; Söderlund, M.; Hoffman, H.J.; Kliner, D.; Koplów, J. Photodarkening measurements in large mode area fibers. *Proc. SPIE* **2007**, *6453*, 64531E. [[CrossRef](#)]
8. Zhao, N.; Xing, Y.B.; Li, J.M.; Liao, L.; Wang, Y.B.; Peng, J.G.; Yang, L.Y.; Dai, N.L.; Li, H.Q.; Li, J.Y. 793 nm pump induced photo-bleaching of photo-darkened Yb³⁺-doped fibers. *Opt. Express* **2015**, *23*, 25272–25278. [[CrossRef](#)]
9. Ponsoda, J.; Sderlund, M.J.; Koplów, J.P.; Koponen, J.J.; Honkanen, S. Photodarkening-induced increase of fiber temperature. *Appl. Opt.* **2010**, *49*, 4139–4143. [[CrossRef](#)]
10. Leich, M.; Fiebrandt, J.; Schwuchow, A.; Jetschke, S.; Unger, S.; Jaeger, M.; Rothhardt, M.; Bartelt, H. Length distributed measurement of temperature effects in Yb-doped fibers during pumping. *Opt. Eng.* **2014**, *53*, 066101. [[CrossRef](#)]
11. Griscom, D.L. Self-trapped holes in glassy silica: Basic science with relevance to photonics in space. *Proc. SPIE* **2011**, *8164*, 816405. [[CrossRef](#)]
12. Shugan, Z.Q.F. *Crystal Color Center Physics*; Shanghai Jiaotong University Press: Shanghai, China, 1989.
13. Rpké, U.; Jetschke, S.; Leich, M. Linkage of photodarkening parameters to microscopic quantities in Yb-doped fiber material. *JOSA B* **2018**, *35*, 3126–3133. [[CrossRef](#)]
14. Jetschke, S.; Leich, M.; Unger, S.; Rpké, U. Combined effect of Yb inversion and pump photons on photodarkening in Yb laser fibers: Experiments and model considerations. *J. Opt. Soc. Am. B* **2019**, *36*, 2438. [[CrossRef](#)]

15. Dong, L.; Archambault, J.L.; Reekie, L.; Russell, P.; Payne, D.N. Photoinduced absorption change in germanosilicate preforms: Evidence for the color-center model of photosensitivity. *Appl. Opt.* **1995**, *34*, 3436–3440. [[CrossRef](#)]
16. Skuja, L. *Defects in SiO₂ and Related Dielectrics: Science and Technology*; Springer Science & Business Media: Berlin/Heidelberg, Germany, 2000; ISBN 978-0-7923-6686-7.
17. Meltz, G.; Morey, W.W.; Glenn, W.H. Formation of Bragg gratings in optical fibers by a transverse holographic method. *Opt. Lett.* **1989**, *14*, 823–825. [[CrossRef](#)]
18. Lee, Y.W.; Broeng, J.; Iii, C.H.; Sinha, S.; Dignonnet, M.; Byer, R.L.; Jiang, S. Measurement of high-photodarkening resistance in phosphate fiber doped with 12% Yb₂O₃. *Proc. SPIE Int. Soc. Opt. Eng.* **2008**, *6873*, 68731D. [[CrossRef](#)]
19. Engholm, M.; Norin, L. Preventing photodarkening in ytterbium-doped high power fiber lasers; correlation to the UV-transparency of the core glass. *Opt. Express* **2008**, *16*, 1260–1268. [[CrossRef](#)]
20. Poyntz-Wright, J.L.; Russell, P.S. Spontaneous relaxation processes in irradiated germanosilicate optical fibres. *Electron. Lett.* **1989**, *25*, 478–480. [[CrossRef](#)]
21. Engholm, M.; Norin, L. Comment on “Photodarkening in Yb-doped aluminosilicate fibers induced by 488 nm irradiation”. *Opt. Lett.* **2008**, *33*, 1217–1218. [[CrossRef](#)]
22. Carlson, C.G.; Keister, K.E.; Dragic, P.D.; Croteau, A.; Eden, J.G. Photoexcitation of Yb-doped aluminosilicate fibers at 250 nm: Evidence for excitation transfer from oxygen deficiency centers to Yb³⁺. *J. Opt. Soc. Am. B* **2010**, *27*, 2087–2094. [[CrossRef](#)]
23. Engholm, M.; Norin, L.; Aberg, D. Strong UV absorption and visible luminescence in ytterbium-doped aluminosilicate glass under UV excitation. *Opt. Lett.* **2007**, *32*, 3352. [[CrossRef](#)] [[PubMed](#)]
24. Engholm, M.; Norin, L.; Hirt, C.; Fredrichthornton, S.T.; Petermann, K.; Huber, G. Quenching processes in Yb lasers: Correlation to the valence stability of the Yb ion. *Solid State Lasers XVIII Technol. Devices* **2009**, *7193*, 486–492. [[CrossRef](#)]
25. Shubin, A.V.; Yashkov, M.V.; Melkumov, M.A.; Smirnov, S.A.; Dianov, E.M. Photodarkening of aluminosilicate and phosphosilicate Yb-doped fibers. In Proceedings of the European Conference on Lasers & Electro-Optics, Munich, Germany, 17–22 June 2007.
26. Paschotta, R.; Tropper, A.C. Cooperative luminescence and absorption in Ytterbium-doped silica fiber and the fiber nonlinear transmission coefficient at $\lambda = 980$ nm with a regard to the Ytterbium ion-pairs’ effect: Comment. *Opt. Express* **2006**, *14*, 6981–6982. [[CrossRef](#)]
27. Kir’yanov Alexander, V.; Barmenkov Yuri, O. Cooperative luminescence and absorption in Ytterbium-doped silica fiber and the fiber nonlinear transmission coefficient at $\lambda = 980$ nm with a regard to the Ytterbium ion-pairs’ effect: Reply. *Opt. Express* **2006**, *14*, 6983–6985. [[CrossRef](#)]
28. Broer, M.M.; Krol, D.M.; Digiovanni, D.J. Highly nonlinear near-resonant photodarkening in a thulium-doped aluminosilicate glass fiber. *Opt. Lett.* **1993**, *18*, 799–801. [[CrossRef](#)] [[PubMed](#)]
29. Frith, G.; Carter, A.; Samson, B.; Faroni, J.; Town, G.E. Mitigation of photodegradation in 790 nm-pumped Tm-doped fibers. *Proc. SPIE* **2010**, *7580*, 9. [[CrossRef](#)]
30. Schaudel, P.G.B.; Prassas, M.; Auzel, F. Cooperative luminescence as a probe of clustering in Yb³⁺ doped glasses. *J. Alloys Compd.* **2000**, *300*, 443–449. [[CrossRef](#)]
31. Jetschke, S.; Unger, S.; Schwuchow, A.; Leich, M.; Fiebrandt, J.; Jäger, M.; Kirchhof, J. Evidence of Tm impact in low-photodarkening Yb-doped fibers. *Opt. Express* **2013**, *21*, 7590–7598. [[CrossRef](#)]
32. Simpson, D.; Gibbs, K.; Collins, S.; Blanc, W.; Dussardier, B.; Monnom, G.; Peterka, P.; Baxter, G. Visible and near infra-red up-conversion in Tm³⁺/Yb³⁺ co-doped silica fibres under 980 nm excitation. *Opt. Express* **2008**, *16*, 13781–13799. [[CrossRef](#)]
33. Bonar, J.R.; Vermelho, M.; McLaughlin, A.J.; Marques, P.; Aitchison, J.S.; Martins-Filho, J.F.; Bezerra, A.G.; Gomes, A.; Araujo, C. Blue light emission in thulium doped silica-on-silicon waveguides. *Opt. Commun.* **1997**, *141*, 137–140. [[CrossRef](#)]
34. Jenouvrier, P.; Boccardi, G.; Fick, J.; Jurdyc, A.M.; Langlet, M. Up-Conversion Emission in Rare Earth-Doped Y₂Ti₂O₇ Sol-Gel Thin Films. *J. Lumin.* **2005**, *113*, 291–300. [[CrossRef](#)]
35. Barber, P.R.; Paschotta, R.; Tropper, A.C.; Hanna, D.C. Infrared-induced photodarkening in Tm-doped fluoride fibers. *Opt. Lett.* **1995**, *20*, 2195–2197. [[CrossRef](#)] [[PubMed](#)]
36. Xing, Y.B.; Liu, Y.; Lin, X.; Chen, G.; Li, J. Bleaching of photodarkening in Tm-doped silica fiber with deuterium loading. *Opt. Lett.* **2020**, *45*, 2534–2537. [[CrossRef](#)]
37. Mejía, E.; Talavera, D.V. Red (632.8-nm) attenuation by a copropagating 1175-nm signal in Tm³⁺-doped optical fibers. *Opt. Eng.* **2007**, *46*, 105001. [[CrossRef](#)]
38. Auzel, F. Upconversion processes in coupled ion systems. *J. Lumin.* **1990**, *45*, 341–345. [[CrossRef](#)]
39. Peretti, R.; Gonnet, C.; Jurdyc, A.M. Revisiting literature observations on photodarkening in Yb³⁺-doped fiber considering the possible presence of Tm impurities. *J. Appl. Phys.* **2012**, *112*, 093511. [[CrossRef](#)]
40. Jolly, A.; Vinçont, C.; Pierre, C.; Bouillet, J. Modelling the competition between photo-darkening and photo-bleaching effects in high-power ytterbium-doped fibre amplifiers. *Appl. Phys. B* **2017**, *123*, 227. [[CrossRef](#)]
41. Nishikawa, H.; Shiroyama, T.; Nakamura, R.; Ohki, Y.; Nagasawa, K.; Hama, Y. Photoluminescence from defect centers in high-purity silica glasses observed under 7.9-eV excitation. *Phys. Rev. B Condens. Matter* **1992**, *45*, 586–591. [[CrossRef](#)]
42. Devine, R.; Arndt, J. Correlated defect creation and dose-dependent radiation sensitivity in amorphous SiO₂. *Phys. Rev. B Condens. Matter* **1989**, *39*, 5132–5138. [[CrossRef](#)]
43. Laperle, P. Etude de lasers a fibre emettant a 480 nm et du phenomene de coloration dans la fibre de ZBLAN dopee au thulium. *Edições Vade-Mécum* **2003**, *86*, 1742003.

44. Laperle, P.; Desbiens, L.; Foulgoc, K.L.; Drolet, M.; Deladurantaye, P.; Proulx, A.; Taillon, Y. Modeling the photodegradation of large mode area Yb-doped fiber power amplifiers. *Spie Lase Lasers Appl. Sci. Eng.* **2009**, *7195*, 550–560. [[CrossRef](#)]
45. Ponsoda, J.J.M.I.; Ye, C.; Koplow, J.P.; Soderlund, M.J.; Koponen, J.J.; Honkanen, S. Analysis of temperature dependence of photodarkening in ytterbium-doped fibers. *Opt. Eng.* **2011**, *50*, 111610.111610.111610.111619. [[CrossRef](#)]
46. Hanna, D.C.; Percival, R.M.; Perry, I.R.; Smart, R.G.; Townsend, J.E.; Tropper, A.C. Frequency upconversion in Tm- and Yb:Tm-doped silica fibers. *Opt. Commun.* **1990**, *78*, 187–194. [[CrossRef](#)]
47. Sun, T.R.; Su, X.Y.; Zhang, Y.H.; Zhang, H.W.; Zheng, Y. Progress and Summary of Photodarkening in Rare Earth Doped Fiber. *Appl. Sci.* **2021**, *11*, 10386. [[CrossRef](#)]
48. Koponen, J.J.; Söderlund, M.J.; Tammela, S.K.T.; Po, H. Photodarkening in ytterbium-doped silica fibers. *Proc. SPIE* **2005**, *5990*, 599008. [[CrossRef](#)]